ELSEVIER

Polymer 40 (1999) 683–694

polymer

Medium strain hysteresis loss of natural rubber and styrene-butadiene rubber vulcanizates: a predictive model

Kamal K. Kar, Anil K. Bhowmick*

Rubber Technology Centre, Indian Institute of Technology, Kharagpur, West Bengal 721 302, India

Received 26 February 1997; revised 30 September 1997; accepted 5 January 1998

Abstract

A model for hysteresis loss of rubber vulcanizates at medium strain (less than 100%) under dynamic condition has been proposed by using Boltzmann superposition principle, statistical theory of rubber elasticity and phenomenological theory. The theory incorporates both experimental and analytical parameters to quantify hysteresis loss. The model with no adjustable parameter has been successfully tested using the experimental results for natural rubber (NR) and styrene-butadiene rubber (SBR) vulcanizates having variations of loading of carbon black, silica, clay, resin and curatives, at various strain rates, strain levels and temperatures. The model is virtually indistinguishable from other well-known models at low strain.

Keywords: Hysteresis loss; Stored energy; Boltzmann superposition principle

1. Introduction

During the past 50 years, mathematical constitutive theory for non-linear large elastic deformation of rubber have been developed on the basis of the statistical mechanics [1–9] and the strain energy density function [10–17]. However, quantitative evaluation of hysteresis loss is not easy. Early attempts of deriving a mathematical expression were not successful due to the complexities of the mathematical formulations and the lack of general guidelines. Since the hysteresis loss in the rubber compound is helpful in understanding the performance of rubber vulcanizates, an effort is made here to quantify the amount of energy dissipated. Experimental studies regarding hysteresis loss of rubber vulcanizates at low and high strains have been reported by various authors: Ferry [18], Mullins et al. [19,20], Payne et al. [21,22], Medalia [23], Meinecke et al. [24] and Roland et al. [25–27]. In spite of its obvious importance there is surprisingly little published work regarding quantitative prediction of hysteresis loss. It has been reported that at low strain, hysteresis loss per cycle is proportional to the loss modulus with a simplifying assumption of linear stress–strain relationship [18]

$$H_y = \frac{\pi}{4}\left(\frac{\mathrm{DSA}}{100}\right)^2 G''(\omega) \tag{1}$$

where DSA is the double strain amplitude or peak to peak displacement in percentage and $G''(\omega)$ is the loss modulus. Yang and Chen [28] calculated energy loss theoretically for linear viscoelastic material under periodic triangular strain loading by using Boltzmann superposition principle and found the results in agreement with Ferry's conclusions [18] that the energy stored during the forward deformation half cycle is completely released during the reverse deformation half cycle. This energy loss in rubber vulcanizates is a complicated phenomena. In our earlier communication [29], we observed that it is a non-linear function of strain amplitudes, strain rates, experimental temperatures and compositional variables like filler loading, types of filler, resin loading, crosslink density and nature of polymers. We have also derived a relationship [30] between heat generation of filled rubber vulcanizates and hysteresis loss, specific heat, thermal conductivity, modulus, filler loading, structure and surface area of the filler, temperature difference between application temperature and glass transition temperature, frequency, temperature difference between wall and environment, stress and stroke amplitude.

Many fundamental questions appear to be unanswered. Is it possible to quantify hysteresis loss at medium strain? What is the degree of dependence of hysteresis loss on strain level, frequency and temperature? Is the model equation different for different elastomers? Does it depend upon the physical properties of the rubber compound, for example, Young's modulus, extensibility or resistance to

* Corresponding author.

0032-3861/98/$ - see front matter
PII: S0032-3861(98)00194-3

tearing? Does repeated deformation play a direct role in causing the failure of rubber to filler network structure? The objective of this paper is to answer some of these questions and to develop a model equation of hysteresis loss with the help of power law derived from Boltzmann superposition principle, statistical theory of rubber elasticity and phenomenological theory. The theory is compared with the experimental results at medium strain uniaxial tension of natural rubber and styrene-butadiene rubber vulcanizates, having variations of loading of carbon black, silica, clay, resin and curatives.

2. Theoretical background

Constitutive models of the large strain, non-linear elastic behavior of rubbery polymers have been in existence for over 50 years; early models included the phenomenological invariant-based approaches such as that developed by Mooney [1] and the statistical mechanics models by investigators such a Flory and Rehner [2], Flory and Erman [3], Ullman [4], Erman [4], Stepto [4], and Arruda and Boyce [5]. Concurrently, statistical mechanics have been developed on the same principle as the rubber elasticity models [6–9]. The expressions thus derived fail to account for the marked dependence of the properties of rubber on strain, strain rates, time and temperature. The actual time dependent response is due to complex chemical and physical interactions involving long chain molecules and fillers. Obviously, these interactions do not have to follow Hooke's law and Newton's viscosity law. Models such as that of Flory and Rehner [2] or the Kuhn and Grün model [9], later investigated by Treloar [8], previously have been shown by Arruda and Boyce [5] not to be predictive of the deformation state dependent response of elastomers at intermediate and large strains. Similarly, the Flory and Erman model [3] requires adjustment of at least one of its parameters in order to explain both uniaxial tension and uniaxial compression data.

Considering the Boltzmann superposition principle [31–34], the state of stress in a rubber-like-material at any given time depends on the deformation history of the material prior to that time. If there is a change of strain at time t of amount $(de/dt)dt$, the stress at some later time τ depends on the product of $(de/dt)dt$ and a function of elapsed time $(\tau - t)$. These products are summed from the beginning of the deformation history of the material to the time at which the stress existing in the material is required. The above can be expressed symbolically by the equation [31]:

$$\phi(S_0) \propto \int_0^{\tau} f(\tau - t)\left(\frac{de}{dt}\right)dt \tag{2}$$

where $\phi(S_0)$ is a stress function having the form $\phi(S_0) = S_0^{K^*}$

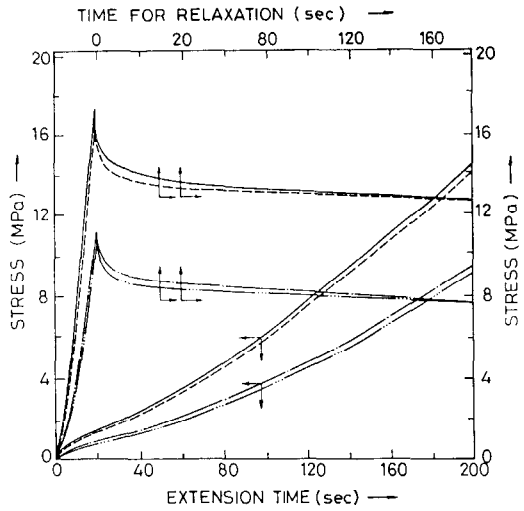

Fig. 1. Effect of extension time and time for stress relaxation on stress at different strain rates for natural rubber vulcanizates (————, 60 phr ISAF black at strain rate of $1.9 \times 10^{-4}\ s^{-1}$; — —, 60 phr ISAF black at strain rate of $1.9 \times 10^{-6}\ s^{-1}$; - · -, 40 phr ISAF black at strain rate of $1.9 \times 10^{-4}\ s^{-1}$; — ··· — ,40 phr ISAF black at strain rate of $1.9 \times 10^{-6}\ s^{-1}$).

where K^* is a constant of the material [31], or,

$$\phi(S_0) = A' \int_0^{\tau} f(\tau - t)\left(\frac{de}{dt}\right)dt \tag{3}$$

where A' is a material constant.

Fig. 1 shows the variation of stress with extension time and time for stress relaxation. As usual, the stress increases with the increase in extension time at constant strain rate and the stress decays with time at constant strain. It may be inferred in line with earlier authors [31] that $f(\tau - t)$ may be represented with sufficient accuracy by the simple function $(\tau - t)^{-m}$ in the case of stress relaxation and $(\tau - t)^{+m}$ in the case of extension time. Although the value of the index m is found to depend on the value of $(\tau - t)$ and level of strain, it may be considered constant over a wide range of values of $(\tau - t)$. Fig. 2 illustrates that stress is a non-linear function

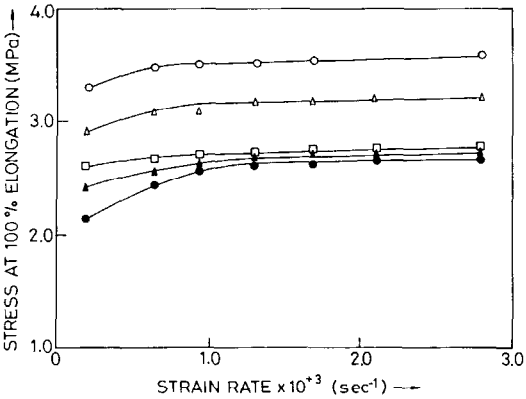

Fig. 2. Effect of strain rates on stress at 100% elongation at different temperatures for 60 phr ISAF filled natural rubber vulcanizate (- ○ -, 25°C; - △ -, 50°C; - □ -, 75°C; - ▲ -, 100°C; and - ● -, 125°C).

of strain rates over a temperature range from 25 to 125°C. The non-linearity of stress with strain rate, stress relaxation and extension time have been demonstrated before [31,33,34]. We have extended the superposition principle by using non-linear functions [35]. Therefore, Eq. (3) now becomes

$$\phi(S_0) = A' \int_0^{\tau} f(\tau - t)^{\pm m} \left(\frac{de}{dt}\right)^n dt \tag{4}$$

The classical theories of a purely entropic elasticity, represented by Eq. (5) lead to the brilliant conclusion that the stress should be directly proportional to the absolute temperature (θ_0) at constant extension ratio (λ). The elastic free energy (W^*) in terms of the conformational entropy along [8] is given by

$$W^* = 1/2\nu_1 k_* \theta_0 (\lambda_1^2 + \lambda_2^2 + \lambda_3^2 - 3) \tag{5}$$

where ν_1 is the number of network chains per unit volume (the crosslink density), k_* Boltzmann's constant and λ_1, λ_2, λ_3 the extension ratios in three directions. Hence,

$$W^* \propto \theta_0 \tag{6}$$

As the stress depends on the temperature, it should be proportional to the temperature rise during deformation of rubber vulcanizates. The above can be expressed as

$$\phi(S_0) \propto d\theta \tag{7}$$

From joint variance, a comparison of Eq. (4), Eq. (7) reveals that

$$\phi(S_0) = -A'' \, d\theta \int_0^{\tau} f(\tau - t)^{\pm m} \left(\frac{de}{dt}\right)^n dt \tag{8}$$

where $-A''$ is a material constant.

From thermodynamics and the calorimetric principles, under quasi-adiabatic condition the temperature rise ($d\theta$) in an extension from the unstrained length (l_0) to the final strain (e_0^*), is given by

$$d\theta = -\frac{\theta_0 l_0}{m'' C_L} \int_0^{e_0^*} \left(\frac{ds'}{dl}\right)_{\theta_0 p'} de \tag{9}$$

where C_L is the specific heat, m'' is mass of the vulcanizate and $(ds'/dl)_{\theta_0 p'}$ is the change of entropy on extension dl at constant temperature θ_0 and pressure p'.

According to the principle of thermodynamics [8], we can write

$$\left(\frac{ds'}{dl}\right)_{\theta_0 p'} = -\left(\frac{ds}{d\theta}\right)_{l,p'} \tag{10}$$

where $(ds/d\theta)_{l,p'}$ is the change of stress with the change of temperature ($d\theta$) at constant length l and pressure p'.

Now combining Eq. (10) into Eq. (9), the temperature rise may be expressed as

$$d\theta = \frac{\theta_0 l_0}{m'' C_L} \int_0^{e_0^*} \left(\frac{ds}{d\theta}\right)_{l,p'} de \tag{11}$$

By substituting Eq. (11) into Eq. (8), we obtain the stress response function as follows:

$$\phi(S_0) = -\frac{A'' \theta_0 l_0}{m'' C_L} \int_0^{e_0^*} \left(\frac{ds}{d\theta}\right)_{l,p'} de \int_0^{\tau} (\tau - t)^{\pm m} \left(\frac{de}{dt}\right)^n dt \tag{12}$$

In order to derive the dependence of stress on temperature (θ_0) under any specified condition (i.e. constant volume or constant pressure), Eq. (13), given below, derived by Treloar [8] may be introduced into Eq. (12)

$$\left(\frac{ds}{d\theta}\right)_{l,p'} = \frac{S_0^*}{\theta_0}\left(1 - \theta_0 \frac{d \ln \bar{r}_0^2}{d\theta} - \frac{\beta\theta_0}{e^3 - 1}\right) \tag{13}$$

In this expression, S_0^* is a function of strain and time, and $\bar{r}_0^2$ is a function of temperature, but is independent of the volume of the specimen. On the other hand, $\bar{r}_i^2$ is a function of the volume of the specimen. β is the volume expansion coefficient.

The mean square chain length, $\bar{r}_i^2$, in the unstrained state is the same as the mean square vector length, $\bar{r}_0^2$, of a corresponding set of free chains. From statistical theory of rubber elasticity [8], $\bar{r}_0^2$ may also be represented as

$$\langle \bar{r}_0 \rangle^2 = \frac{\int_0^{\infty} r^2 \omega(r) \, dr}{\int_0^{\infty} \omega(r) \, dr} \tag{14}$$

The radial distribution function $\omega(r)$ in the non-Gaussian region was first derived by Kühn and Grün [8] and given by

$$\omega(r) = C^* \exp\left\{ -n' \left[\frac{r\mathcal{L}^{-1}\left(\frac{r}{n'l'}\right)}{n'l'} + \ln \frac{\mathcal{L}^{-1}\left(\frac{r}{n'l'}\right)}{\sinh \mathcal{L}^{-1}\left(\frac{r}{n'l'}\right)} \right] \right\} \tag{15}$$

where C^* is a normalization constant, $\mathcal{L}^{-1}$ is the inverse Langevin function and n' is the number of monomer units in a polymer chain, each of which has a length l'.

From Eqs (14) and (15), we obtain

$$\langle \bar{r}_0 \rangle^2 = f(n'l') \tag{16}$$

Taking logarithms and differentiation of Eq. (16) with respect to temperature with a simplifying assumption that l' is independent of temperature (θ_0) due to the very low thermal expansion coefficient of the molecules in the cross-linked state, we have

$$\frac{d \ln \langle \bar{r}_0 \rangle}{d\theta} = \frac{d \ln f(n'l')}{d\theta} = 0 \tag{17}$$

Comparison of Eq. (13) with Eq. (17) reveals that

$$\left(\frac{ds}{d\theta}\right)_{p',l} = \frac{S_0^*}{\theta_0}\left(1 - \frac{\beta\theta_0}{e^3 - 1}\right) \tag{18}$$

Now introducing Eq. (18) into Eq. (12), we therefore write

$$\phi(S_0) = -\frac{A''\theta_0 l_0}{m''C_L}\int_0^{e_0^*}\frac{S_0^*}{\theta_0}\left(1-\frac{\beta\theta_0}{e^3-1}\right)de\int_0^{\tau}(\tau-t)^{\pm m}\left(\frac{de}{dt}\right)^n dt \tag{19}$$

If the strain is a simple harmonic function of time such that

$$e_0^*(t) = e_0^* \sin\omega t \tag{20}$$

then stress becomes

$$S_0^*(t) = S_0^{**}\sin(\omega t+\delta) \tag{21}$$

where ω is the frequency and δ is the phase angle. In this case, we assume that phase angle is independent on strain amplitude (at intermediate strain, phase angle varies slightly with strain amplitude).

Analysis of the dynamic response by using sine functions is not a problem, but the use of complex functions gives easier mathematical formulation and better understanding of the process of deformation. On the basis of complex variables, the input and the output function can be represented as

$$\left.\begin{aligned} e_0^*(t) &= e_0^*\exp^{i\omega t}\\ S_0^*(t) &= S_0^{**}\exp^{i(\omega t+\delta)}\end{aligned}\right\} \tag{22}$$

Now performing the differentiation of Eq. (22) with respect to time (t), then substituting into Eq. (19) and rearranging, we can write

$$\phi(S_0) = -\frac{A''l_0\{e_0^*(\omega)\}^n(i)^n(\omega)^n}{m''C_L}\int_0^{e_0^*}S_0^{**}\exp^{i(\omega t+\delta)}\cdot\left[1-\frac{\beta\theta_0}{e^3-1}\right]de\int_O^{\tau}(\tau-t)^{\pm m}\exp^{ni\omega t}dt \tag{23}$$

where S_0^{**} is a function of strain. To find out the stress at any point, we have to replace S_0^{**} in terms of strain. For this purpose we apply continuum theory of finite deformation.

Now applying the continuum theory of finite deformation, the stress–strain equation of homogeneous isotropic and elastic materials such as vulcanized rubber can be derived from the strain energy density function, W_*, which is the elastic energy stored in a deformed body.

According to Ogden [8], the strain energy for incompressible material can be written as

$$W_* = W(I_1)+W(I_2) = \sum_{i'=1}^{3}\sum_{j=1}^{m'}(C_j/b_j)\left(\lambda_{i'}^{b_j}-1\right) \tag{24}$$

where C_j and b_j are material coefficients; λ_1, λ_2 and λ_3 are the principal extension ratios; and m' is a material constant.

In the case of homogeneous uniaxial deformation, the stress S_0^{**} can be derived from W_*

$$S_0^{**} = \sum_{j=1}^{m'}C_j\left(\lambda^{b_j-1}-\lambda^{-(1+0.5b_j)}\right) \tag{25}$$

where λ is the uniaxial stretch

$$= 1+\frac{dl}{l_0} \tag{26}$$

$$= 1+e$$

A comparison of Eq. (23) with Eqs. (25) and (26) reveals that

$$\phi(S_0) = A(i)^n\int_0^{e_0^*}\sum_{j=1}^{m'}C_j\left[(1+e)^{b_j-1}-(1+e)^{-(1+0.5\,b_j)}\right]\cdot\exp^{i(\omega t+\delta)}\left[1-\frac{\beta\theta_0}{e^3-1}\right]de\int_0^{\tau}(\tau-t)^{\pm m}\exp^{ni\omega t}dt \tag{27}$$

where

$$A = -\frac{A''l_0\{e_0^*(\omega)\}^n}{m''C_L}$$

Now, we assume that stress (S_0) is a non-linear function of $\phi(S_0)$. The above Eq. (27) can be represented as

$$S_0^{K^*} = A(i)^n\int_0^{e_0^*}\sum_{j=1}^{m'}C_j\left[(1+e)^{b_j-1}-(1+e)^{-(1+0.5\,b_j)}\right]\cdot\exp^{i(\omega t+\delta)}\left[1-\frac{\beta\theta_0}{e^3-1}\right]de\int_0^{\tau}(\tau-t)^{\pm m}\exp^{ni\omega t}dt \tag{28}$$

We design the experiment in the following manner. We elongate the test piece at a certain strain rate up to e_{k+1}. Then, the test piece is retracted at the same train rate. The stress–strain curve obtained is represented in Fig. 3.

The complete cycle consists of two segments: a deformation segment from time $(\nu-1)\tau'+t_{k-1}$ to $(\nu-1)\tau'+t_k$ and a recovery segment from $(\nu-1)\tau'+t_{k''-1}$ to $(\nu-1)\tau'+t_{k''}$.

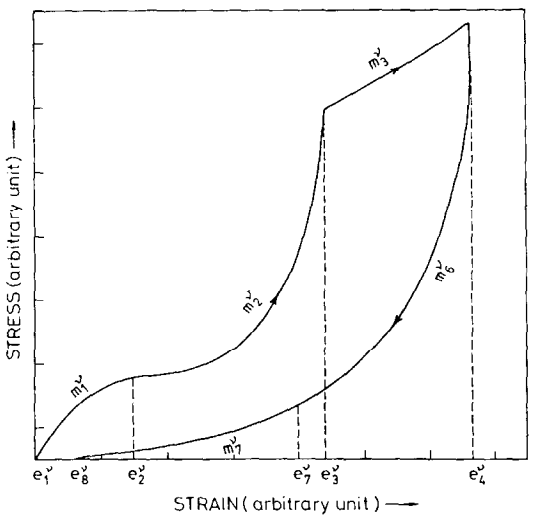

Fig. 3. Schematic representation of typical stress–strain hysteresis loop curve for an arbitrary rubber vulcanizate.

ν represents the number of cycles which varies from 1 to $N'+1$ and k is a number that varies from 1 to k' and k'' from $k'+1$ to $k'+k_2$.

It is observed that the magnitude of m varies with time in the following manner. Between $(\nu-1)\tau'+t_{k-1}$ to $(\nu-1)\tau'+t_k$, let m have the value m_k^ν and between $(\nu-1)\tau'+t_{k''-1}$ to $(\nu-1)\tau'+t_{k''}$ have the values $m_{k''}^\nu$. In this time interval the strain value varies in the following manner: e_k^ν to e_{k+1}^ν in the time interval $(\nu-1)\tau'+t_{k-1}$ to $(\nu-1)\tau'+t_k$ and $e_{k''}^\nu$ to $e_{k''+1}^\nu$ in the time interval $(\nu-1)\tau'+t_{k''-1}$ to $(\nu-1)\tau'+t_{k''}$.

Considering Eq. (28), the stress at any cycle and at any point may be represented as

$$
\begin{aligned}
S_0^{K^*} = {} & \sum_{k=1}^{k'}\sum_{\nu=1}^{N'+1} A_k^\nu (i)^n \int_{e_k^\nu}^{e_{k+1}^\nu} \sum_{j=1}^{m'} C_j\left[(1+e)^{b_j-1}\right. \\
& \left. -(1+e)^{-(1+0.5\,b_j)}\right]\cdot \exp^{i(\omega t+\delta)}\left[1-\frac{\beta\theta_0}{e^3-1}\right] \\
& \times \mathrm{d}e \int_{(\nu-1)\tau'+t_{k-1}}^{(\nu-1)\tau'+t_k} (t-t_{k-1})^{m_k^\nu} \exp^{ni\omega t}\,\mathrm{d}t \\
& + (-1)^n \sum_{k''=k'+1}^{k'+k_2}\sum_{\nu=1}^{N'+1} A_{k''}^\nu (i)^n \int_{e_{k''}^\nu}^{e_{k''+1}^\nu} \sum_{j=1}^{m'} C_j\left[(1+e)^{b_j-1}\right. \\
& \left. -(1+e)^{-(1+0.5\,b_j)}\right]\cdot \exp^{i(\omega t+\delta)}\left[1-\frac{\beta\theta_0}{e^3-1}\right]\mathrm{d}e \\
& \cdot \int_{(\nu-1)\tau'+t_{k''-1}}^{(\nu-1)\tau'+t_{k''}} (t-t_{k''-1})^{-m_{k''}^\nu} \exp^{ni\omega t}\,\mathrm{d}t
\end{aligned}
\tag{29}
$$

The first term on the right hand side of Eq. (29) portrays the stress during the deformation part of the cycle and the second term represents the recovery part of the cycle.

3. Hysteresis loss or energy dissipation

Since the energy loss per unit time t per unit volume of a material is the product of the instantaneous stress and the rate of strain i.e.

$$\dot{H}_y = S_0(t)\dot{e}(t) \tag{30}$$

the total hysteresis loss per unit volume in a deformation cycle is represented by

$$H_y = \oint S_0(t)\dot{e}(t)\,\mathrm{d}t \tag{31}$$

For the first cycle with time from zero up to $2t_k$, the total hysteresis loss per unit volume is given by

$$H_y = \int_0^{t_k} S_0(t)\dot{e}(t)\,\mathrm{d}t + \int_{t_k}^{2t_k} S_0(t)\dot{e}(t)\,\mathrm{d}t \tag{32}$$

The equations for the hysteresis loop after the first cycle can be readily derived by further application of superposition principle.

The hysteresis loss per unit volume in the steady state i.e. in the Nth cycle is given by

$$H_y = \int_{N\tau'+t_{k-1}}^{N\tau'+t_k} S_0(t)\dot{e}(t)\,\mathrm{d}t + \int_{N\tau'+t_{k''-1}}^{N\tau'+t_{k''}} S_0(t)\dot{e}(t)\,\mathrm{d}t \tag{33}$$

For complex mathematical formulation, it is very difficult to find out H_y from Eq. (32). As an approximation, we therefore consider the integral above (Eq. (31)) to be written as follows

$$\left[H_y\right]^{k^*} = \oint S_0^{K^*}(t)\,\mathrm{d}e \tag{34}$$

Substituting Eq. (29) into Eq. (34) with a simplifying assumption ($m=1$, $j=1$, $n=1$) of non-linear function of stress–strain rate and extension or retraction time, we find that the hysteresis loss per unit volume for complete cycle is

$$
\begin{aligned}
\left[H_y\right]^{K^*} = {} & \frac{\pi M^* \sin\delta}{\omega}\,\beta\theta_0\left[\frac{e_1^4}{48\beta\theta_0} + \sum_{n''=1}^{\infty}\frac{e_1^{n''+1}}{(n'')^2}\right. \\
& \left. -\frac{e_1^{n''+1}}{n''(n''+1)^2} - \frac{e_1^{n''+1}}{n''(n''+1)}\right]
\end{aligned}
\tag{35}
$$

where $M^* = \frac{0.013A''l_0C_1}{3C_1} = \text{Constant}$

The constant M^* depends on C_1, the material coefficients. As C_1 is constant for a given vulcanizate, so M^* is also constant (but not a universal constant).

The energy stored per unit volume in a quarter cycle is

$$
\begin{aligned}
\left[E_{\text{Energy stored}}\right]^{K^*} = {} & \frac{M^*\cos\delta}{2\omega}\,\beta\theta_0 \\
& \times\left[\frac{e_1^4}{48\beta\theta_0} + \sum_{n''=1}^{\infty}\frac{e_1^{n''+1}}{(n'')^2} - \frac{e_1^{n''+1}}{n''(n''+1)^2} - \frac{e_1^{n''+1}}{n''(n''+1)}\right]
\end{aligned}
\tag{36}
$$

The ratio of dissipated to stored energy per cycle is

$$\left[\frac{E_{\text{Energy dissipated}}}{E_{\text{Energy stored}}}\right]^{K^*} = 2\pi\tan\delta \tag{37}$$

At very low strain (where $K^*=1$), Eq. (34) reduces to

$$\left[H_y\right] = \frac{\pi G''(\omega)e_1^2}{4} \tag{38}$$

where

$$G''(\omega) = \frac{M^*\sin\delta}{\omega}\,\beta\theta_0$$

Similarly, Eq. (36) gives

$$E_{\text{Energy stored}} = \frac{G'(\omega)e_1^2}{8} \tag{39}$$

where

$$G'(\omega) = \frac{M^*\cos\delta}{\omega}\,\beta\theta_0$$

Table 1
Formulation of mixes

Mix number	A_i	B_i	C_i	D_i	E_i	F_i	G_i	H_i	I_i	J_i	K_i	L_i
NR	100	0	100	0	100	0	100	0	100	0	100	0
SBR	0	100	0	100	0	100	0	100	0	100	0	100
ZnO	5.0	5.0	5.0	5.0	5.0	5.0	5.0	5.0	5.0	5.0	5.0	5.0
Steric acid	2.0	2.0	2.0	2.0	2.0	2.0	2.0	2.0	2.0	2.0	2.0	2.0
TMQ	1.5	1.5	1.5	1.5	1.5	1.5	1.5	1.5	1.5	1.5	1.5	1.5
6PPD	1.5	1.5	1.5	1.5	1.5	1.5	1.5	1.5	1.5	1.5	1.5	1.5
ISAF black	$A_{i=0-60}$	$B_{i=0-60}$	40	40	40	40	40	0	0	0	0	0
Silica	0	0	0	0	0	0	0	0	20	20	0	0
Clay	0	0	0	0	0	0	0	0	0	0	20	20
Aromatic oil	5.0	5.0	5.0	5.0	5.0	5.0	0	0	0	0	0	0
Si-69	0	0	0	0	0	0	0	0	2.0	2.0	0	0
Resin	0	0	$C_{i=0-40}^{j=0-20}$	$D_{i=0-40}^{j=0-20}$	0	0	10	10	0	0	0	0
BSM	0.8	0.8	0.8	0.8	$E_{i=1-4}$	$F_{i=1-3}$	0.8	0.8	0.8	0.8	0.8	0.8
Sulfur	2.5	2.5	2.5	2.5	$E_{i=1-4}$	$F_{i=1-3}$	2.5	2.5	2.5	2.5	2.5	2.5
PVI	0.5	0.5	0.5	0.5	0.5	0.5	0.5	0.5	0.5	0.5	0.5	0.5

$A_{i=0-60}$: A_0, A_{20}, A_{40}, A_{60}, suffix indicates loading of filler
$B_{i=0-60}$: A_0, A_{20}, A_{40}, A_{60}, suffix indicates loading of filler
$C_{i=0-40}^{j=0-20}$: C_0^0, C_0^{10}, C_{40}^0, C_{40}^{20}, i indicates loading of filler and j indicates loading of resin~
$D_{i=0-40}^{j=0-20}$: D_0^0, D_0^{10}, D_{40}^0, D_{40}^{20}, i indicates loading of filler and j indicates loading of resin
$E_{i=1-4}$: E_1 (BSM/S = 0.8/2.5), E_2 (BSM/S = 1.5/1.5), E_3(BSM/S = 1.0/1.0), E_4(BSM/S = 3.0/3.0)
$F_{i=1-4}$: F_1 (BSM/S = 0.8/2.5), F_2 (BSM/S = 1.5/1.5), F_3(BSM/S = 1.0/1.0), F_4(BSM/S = 3.0/3.0)

The ratio of dissipated to stored energy is

$$\left[\frac{E_{\text{Energy dissipated}}}{E_{\text{Energy stored}}}\right] = [2\pi \tan \delta] \tag{40}$$

where

$$\tan \delta = \frac{G''(\omega)}{G'(\omega)}$$

Eqs. (38)–(40) agree with Eqs. (24)–(26) in chapter 5 of reference [36].

4. Experimental

The formulations of the various mixes are given in Table 1. The nature of polymers (mixes A_i to L_i), the loading of filler (mixes (A_i and B_i), the nature of filler (mixes I_i, J_i, K_i and L_i), the loading of resin (mixes C_i and D_i) and the crosslink density (mixes E_i, F_i, G_i and H_i) were varied. Natural rubber (RMA-4), SBR-1502, stearic acid, Si-69 (Degussa, AG), silica and aromatic oil were supplied by Birla Tyres Ltd., Balasore. ISAF (N220) was supplied by Phillips Carbon Black Ltd., Durgapur. Zinc oxide and clay were obtained from the local market. High styrene resin and sulfur were supplied by Bengal Waterproof Ltd., Panihati. Polymerised 1,2-dihydro 2,2,4-trimethyl quinoline (TMQ), N-(1,3-dimethylbutyl)-N′-Phenyl-p-phenylene-diamine (6-PDD), N-cyclohexylthiophthalimide (PVI) and 2-(4-morpholinyl mercapto)-benzthiazole sulphenamide (BSM) were supplied by ICI Ltd., Rishra.

5. Mixing

The ingredients were mixed with rubber on a two-roll mill (0.15 × 0.33 m, Schwabenthan, Germany) at a temperature of 50°C and a friction ratio 1:1.1.

6. Curing

The curing characteristics of the mixes were evaluated from a Rheometer R-100 according to ASTM D-1084-81. The moulding of the tensile sheets was carried out at a temperature of 150°C, 4 MPa pressure and optimum cure time (t_{90} in minute) using David Bridge Press, Castleton, Rochdale, England.

7. Measurements

7.1. Hysteresis

Medium strain hysteresis loss is defined as the energy dissipated in stretching, when the specimens were deformed to strain level less than 100%. Hysteresis loss was determined on the tensile dumbbells (ASTM D-412-80, type 2 die) over a range of temperatures (25 to 100°C) and strain rates (1.9×10^{-3} s^{-1} to 9.5×10^{-2} s^{-1}) and extensions 1 to 100% using Zwick Universal Testing machine 1445 equipped with an environmental chamber. The samples were mounted in mechanical clamps 44 mm apart and the

cross-head was adjusted to give zero tension. The temperature was controlled to ±0.5°C. The samples were preconditioned in the Zwick heating chamber for 10 min before testing. For the purpose of obtaining hysteresis energy loss continuously, the stress–strain curves were recorded on tape and fed into the attached computer. The measurements were continued up to eight cycles. Experimental results were reproducible within ∓1%.

7.2. Dynamic mechanical properties

The elastic modulus (E'), loss modulus (E'') and loss tangent (tan δ) were calculated from hysteresis loop by methods described elsewhere [37]. The loops were obtained from the stress–strain measurements (forward and retraction curves). At high deformation, the hysteresis loops were not ellipsoidal, instead appeared as banana-shaped loops. The skewed loop was transformed into a nearly elliptical loop by plotting true stress $[(F'/A_0)(1+e)]$ in place of engineering stress $[(F'/A_0)]$ as a function of strain, where F' is the force, A_0 is the original cross-sectional area and e is the strain. It is estimated that the maximum errors in the dynamic mechanical properties were about ∓ 2%

7.3. Young's modulus

Young's modulus was measured from the initial slope (below 50% elongation) of the stress–strain curves in a Zwick UTM model 1445 according to ASTM D 412-80 over a range of temperatures from 25 to 100°C and strain rates 1.9×10^{-3} s^{-1} to 9.5×10^{-2} s^{-1}. Experimental results were reproducible within ∓ 1%.

7.4. Volume expansion coefficient

The values of volume expansion coefficient of rubber were taken from the literature [38].

8. Results and discussion

The result is a fully three-dimensional variable based constitutive model of rubber elasticity in which the rubber modulus and limiting network extensibility properties are needed to be completely characterized for the hysteresis loss of rubber vulcanizates. The quantitative prediction of hysteresis loss using Eq. (35) would involve the measurement of K^*, M^*, volume expansion coefficient (β), and phase angle (δ) at a frequency (ω) and operating temperature (θ_0). For the sake of convenience, we define another parameter M^{**}, as follows:

$$M^{**} = [M^*]^{1/K^*} \tag{41}$$

Hysteresis loss was performed at different strain levels, in order to obtain the material constants K^* and M^{**}. The constants were evaluated by curve fitting using known

Table 2
Material constants K^* and M^{**}[a] of NR and SBR vulcanizates at 25°C

		First cycle		Fourth cycle				First cycle		Fourth cycle	
Strain rate (s^{-1}) × 10^{+2}		1.9	9.5	1.9	9.5			1.9	9.5	1.9	9.5
A_0	K^*	1.75	1.75	1.75	1.75	B_0	K^*	1.75	1.75	1.75	1.75
	M^{**}	0.06	0.10	0.04	0.06		M^{**}	0.09	0.20	0.06	0.13
A_{20}	K^*	1.75	1.75	1.75	1.75	B_{20}	K^*	1.75	1.75	1.75	1.75
	M^{**}	0.16	0.36	0.10	0.22		M^{**}	0.16	0.45	0.10	0.32
A_{40}	K^*	1.75	1.75	1.75	1.75	B_{40}	K^*	1.75	1.75	1.75	1.75
	M^{**}	0.28	0.63	0.18	0.40		M^{**}	0.32	0.63	0.22	0.56
A_{60}	K^*	1.75	1.75	1.75	1.75	A_{60}	K^*	1.75	1.75	1.75	1.75
	M^{**}	0.55	1.26	0.45	1.0		M^{**}	0.56	1.26	0.25	0.80
C_0^{10}	K^*	1.75	1.75	1.75	1.75	D_0^{10}	K^*	1.75	1.75	1.75	1.75
	M^{**}	0.06	0.07	0.04	0.05		M^{**}	0.10	0.32	0.06	0.16
D_{40}^{10}	K^*	1.75	1.75	1.75	1.75	D_{40}^{10}	K^*	1.75	1.75	1.75	1.75
	M^{**}	0.32	0.80	0.20	0.40		M^{**}	0.32	1.00	0.24	0.56
C_{40}^{20}	K^*	1.75	1.75	1.75	1.75	D_{40}^{20}	K^*	1.75	1.75	1.75	1.75
	M^{**}	0.33	0.79	0.22	0.56		M^{**}	0.32	0.89	0.18	0.63
E_1	K^*	1.75	1.75	1.75	1.75	F_1	K^*	1.75	1.75	1.75	1.75
	M^{**}	0.32	0.63	0.22	0.45		M^{**}	0.22	0.46	0.18	0.36
E_2	K^*	1.75	1.75	1.75	1.75	F_2	K^*	1.75	1.75	1.75	1.75
	M^{**}	0.28	0.71	0.18	0.50		M^{**}	0.25	0.80	0.18	0.56
E_4	K^*	1.75	1.75	1.75	1.75	F_3	K^*	1.75	1.75	1.75	1.75
	M^{**}	0.50	1.26	0.30	0.89		M^{**}	0.25	0.80	0.18	0.56
I_1	K^*	1.75	1.75	1.75	1.75	J_1	K^*	1.75	1.75	1.75	1.75
	M^{**}	0.10	0.22	0.07	0.16		M^{**}	0.18	0.56	0.14	0.36
K_1	K^*	1.70	1.75	1.70	1.70	L_1	K^*	1.75	1.75	1.75	1.75
	M^{**}	0.13	0.32	0.07	0.16		M^{**}	0.20	0.60	0.18	0.41

[a]The unit of material constant M^{**} is MPa s$^{-1/2}$

Table 3
Material constants K^* and M^{**}[a] of SBR vulcanizates at 100°C

		First cycle			Fourth cycle		
Strain rate (s^{-1}) × 10^{+2}		0.19	1.9	9.5	0.19	1.9	9.5
(B_{20})	K^*	1.75	1.75	1.75	1.75	1.75	1.75
	M^{**}	0.05	0.18	0.32	0.02	0.08	0.20
(F_1)	K^*	1.75	1.75	1.75	1.75	1.75	1.75
	M^{**}	0.06	0.11	0.22	0.03	0.10	0.12
(F_2)	K^*	1.75	1.75	1.75	1.75	1.75	1.75
	M^{**}	0.03	0.07	0.11	0.01	0.04	0.10
(J_1)	K^*	1.75	1.75	1.75	1.75	1.75	1.75
	M^{**}	0.07	0.28	0.63	0.04	0.18	0.40
(L_1)	K^*	1.75	1.75	1.75	1.75	1.75	1.75
	M^{**}	0.05	0.18	0.32	0.02	0.08	0.20

[a]The unit of material constant M^{**} is MPa $s^{-1/2}$

values of hysteresis loss, frequency, phase angle, volume expansion coefficient and temperature. Once characterized using the single medium deformation experiment, the hysteresis loss in other deformation state may then be predicted without adjusting any model parameter. Tables 2 and 3 describe the values of K^* and M^{**} for the vulcanizates A_i and L_i.

It is apparent from Tables 2 and 3 that the material constant M^{**} is a function of strain rates, number of cycles, temperatures and material compositions. The material constant (M^{**}) increases with increase of strain rate but decreases with increase of temperature and number of cycles. At multiple cycles, the material constant of the rubber decreases and becomes almost constant from the fourth cycle onward. This is ascribed to the disentanglement and reorientation of long chain rubber molecules during stretching along the direction of major axis. The material constant is in general higher for SBR vulcanizates (except F_1) due to the reasons described later. It is important, therefore, that increment or decrement with reference to material constant, M^{**}, due to the varying compositions of rubber vulcanizates and operating variables should be correlated with the basic properties of the rubber vulcanizates.

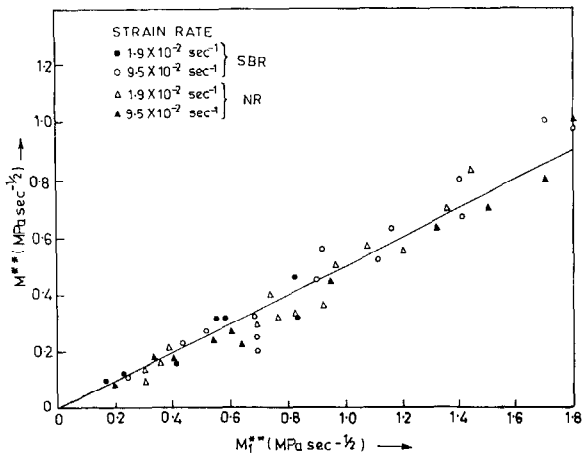

Fig. 4. Material constant M^{**}, versus another material constant M_1^{**}.

Hence, another material constant M_1^{**}, may be defined as the product of Young's modulus and square root of the strain rate. Fig. 4 plots the values of material constant M^{**} against the material constant M_1^{**} for both NR and SBR vulcanizates over a range of strain rates, number of cycles, temperatures and material compositions. The variation in compositions includes nature and level of filter, resin and vulcanization system. From Fig. 4 the following equation is derived

$$M^{**} = A^* M_1^{**} \tag{42}$$

The value of A^* has been found to be 0.5. An excellent correlation is observed between the material constant M^{**} and M_1^{**}. A plot of the material constant in Fig. 4 shows that model equation of hysteresis loss is a non-linear function of material properties i.e. Young's modulus.

On the other hand, the other material constant, K^*, is independent of number of cycles, material compositions, temperatures and strain rates.

The variations of loss tangent (tan δ) with DSA at different strain rates are shown in Fig. 5. At small strain, tan δ is small. As the strain amplitude is increased, tan δ passes through a maximum value. The loss tangent increases

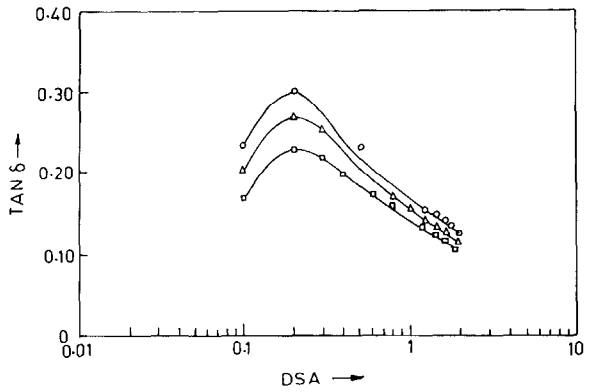

Fig. 5. Effect of double strain amplitude on loss tangent on a semilog plot: fourth cycle in different strain rates for 40 phr ISAF filled NR vulcanizates (-○-, 1.9×10^{-3} s^{-1}; - △ -, 1.9×10^{-2} s^{-1}; and - □ -, 9.5×10^{-2} s^{-1}).

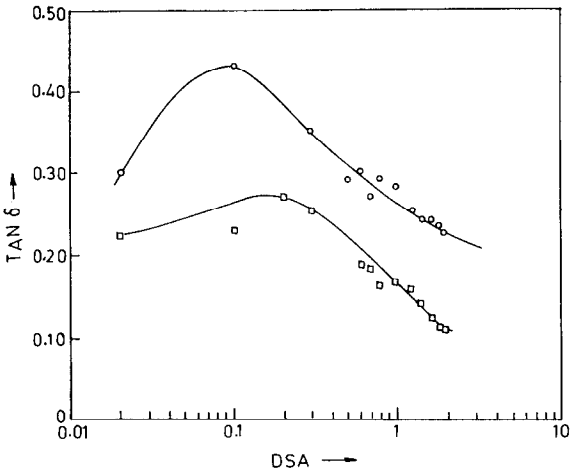

Fig. 6. Effect of DSA on loss tangent for 40 phr ISAF filled NR vulcanizates at 9.5 × 10^{-2} s^{-1} strain rate (- ○ -, first cycle; and - □ -, fourth cycle).

with the strain rates at any double strain amplitude. At low DSA, the agglomerate structure of the carbon black does not break down. The high energy dissipation in the region of the maxima is the result of frictional force due to agglomeration and deagglomeration of the filler. This mechanism decreases at high strain amplitudes where the agglomerated structures break down. Fig. 6 illustrates the plot of the loss tangent versus DSA at first cycle and fourth cycle on a semilogarithmic plot. The nature of this curve is almost similar to that shown in Fig. 5. It may be noted that tan δ_{max} value appears at 0.2 DSA. These results are in agreement with the literature values [36]. Thus, we can infer that a standard analysis [37] of the distorted hysteresis loops obtained at large DSA is sufficiently accurate for our analysis.

The hysteresis loss at different temperatures, frequencies and strain levels have been computed at the desired cycle. The results regarding hysteresis loss of first cycle are plotted against DSA for both NR and SBR vulcanizates shown in Figs. 7 and 8. The experimental values are also shown in the same curve. The hysteresis loss increases with an increase in strain level due to more breakdown of rubber-filler agglomerate structures and higher coefficient of friction between molecules. At 0.6 DSA, there is a sharp increase of hysteresis loss due to the breakdown of rubber-filler agglomerate structures. The theoretical values calculated by Eq. (35), are in good accord with the experimental values (within ±1%). The model equation also reveals that the degree of dependence of strain level on hysteresis loss is a highly non-linear function.

The decrease of hysteresis loss with an increase in temperature due to the decrease in $M^{**}(M^{**} = [M^*]^{1/K^*})$ is reflected in our model Eq. (35). This is attributed to the decrease of coefficient of friction between the molecules, melting of immobilized rubber shell around the filler surface and decrease of rubber-filler interaction.

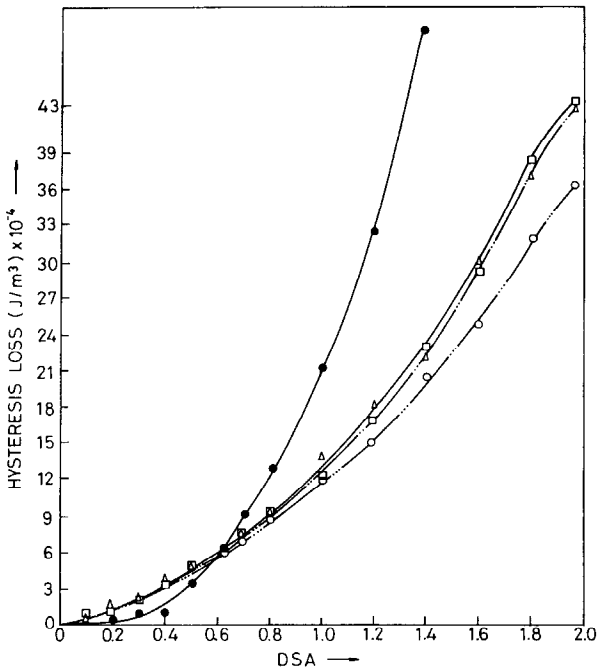

Fig. 7. (a) Effect of double strain amplitude and hysteresis loss for 40 phr ISAF filled NR vulcanizates. Theoretical prediction: J. D. Ferry (- ● -, at strain rate 9.5×10^{-2} s^{-1}) and our model Eq. (35) at different strain rates: – ··· –, 1.9×10^{-3} s^{-1}; –· ·–, 1.9×10^{-2} s^{-1}; ———, 9.5×10^{-2} s^{-1}. (b) Experimental results at different strain rates (○, 1.9 × 10^{-3} s^{-1}; △, 1.9 × 10^{-2} s^{-1}; and □, 9.5 × 10^{-2} s^{-1}).

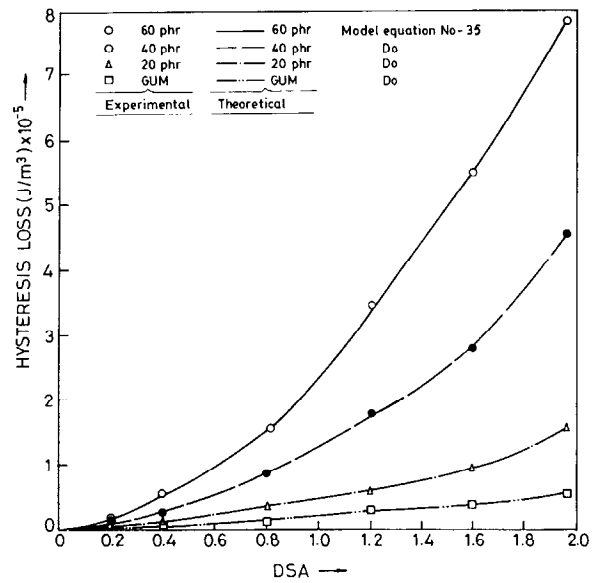

Fig. 8. Effect of double strain amplitude on hysteresis loss at strain rate 1.9 × 10^{-2} s^{-1} for SBR vulcanizates having variation of loading of carbon black.

The model equation shows that hysteresis loss per unit volume and per cycle is inversely non-linear function of frequency. But hyteresis loss per unit volume and per second ($\dot{H}_y$) when the frequency is

$$\dot{f} = \frac{\omega}{2\pi}\,\text{Hz}$$

$$[\dot{H}_y] = \left[\frac{\pi M^* \sin\delta}{\omega}\beta\theta_0\left[\frac{e_1^4}{48\beta\theta_0} + \sum_{n''=1}^{\infty}\frac{e_1^{n''+1}}{(n'')^2} - \frac{e_1^{n''+1}}{n''(n''+1)^2} - \frac{e_1^{n''+1}}{n''(n''+1)}\right]\right]^{1/K^*}\left[\frac{\omega}{2\pi}\right] \tag{43}$$

Rearranging Eq. (43), we obtain

$$[\dot{H}_y] = \frac{1}{2}\left[\frac{\pi M^* \sin\delta}{\omega}\beta\theta_0\left[\frac{e_1^4}{48\beta\theta_0} + \sum_{n''=1}^{\infty}\frac{e_1^{n''+1}}{(n'')^2} - \frac{e_1^{n''+1}}{n''(n''+1)^2} - \frac{e_1^{n''+1}}{n''(n''+1)}\right]\right]^{1/K^*}\left[\frac{\omega}{\pi}\right]^{1-1/K^*} \tag{44}$$

Substituting the value of K^* from Tables 2 and 3 into Eq. (44), we obtain

$$[\dot{H}_y] = \frac{1}{2}\left[\frac{\pi M^* \sin\delta}{\omega}\beta\theta_0\left[\frac{e_1^4}{48\beta\theta_0} + \sum_{n''=1}^{\infty}\frac{e_1^{n''+1}}{(n'')^2} - \frac{e_1^{n''+1}}{n''(n''+1)^2} - \frac{e_1^{n''+1}}{n''(n''+1)}\right]\right]^{0.57}\left[\frac{\omega}{\pi}\right]^{0.43} \tag{45}$$

Model Eq. (45) reveals that hysteresis loss per second increases in proportion with frequency of deformation. It was also reported in earlier papers [29,31].

The hysteresis loss has also been calculated using Ferry's equation [18] (Eq. (1)), shown in the same Fig. 7. At low DSA, there is some agreement, but divergence is observed at medium DSAs. Our calculation shows better correspondence at low and medium DSAs.

It is understood from Tables 2 and 3 and Fig. 4 that model equation regarding quantitative evaluation of hysteresis loss in any deformation state without adjusting any model parameter, is independent of the nature of elastomer and vulcanizates having variation of compositions.

9. Conclusions

In this paper we have developed a constitutive model for quantitative prediction of hysteresis loss of rubber vulcanizates at medium strains (1–100%). The relationship relating hysteresis loss with the material properties and the operating parameters i.e. material constants, strain levels and temperatures, has been developed by using power law derived from Boltzmann superposition principle, statistical theory of rubber elasticity and phenomenological theory. The model uses the experimentally measured material constant of a deforming elastomer as a state dependent variable and the rubbery modulus of the elastomer to simulate the nominal stress response associated with the imposed deformation state. The following conclusions are made.

1. Hysteresis loss per unit volume and per cycle in a rubber vulcanizate is a highly non-linear function of strain level as follows:

$$[\dot{H}_y]^{K^*} = \frac{\pi M^* \sin\delta}{\omega}\beta\theta_0\left[\frac{e_1^4}{48\beta\theta_0} + \sum_{n''=1}^{\infty}\frac{e_1^{n''+1}}{(n'')^2} - \frac{e_1^{n''+1}}{n''(n''+1)^2} - \frac{e_1^{n''+1}}{n''(n''+1)}\right]$$

2. The model equation is shown to be successful in describing the increase of hysteresis loss with increase of strain levels (1–100%) and decrease of hysteresis loss with increase of temperatures for both natural rubber and styrene-butadiene rubber networks.
3. Hysteresis loss can be calculated at any strain levels (1–100%), frequencies and temperatures for natural rubber and styrene-butadiene rubber vulcanizates, having variations of loading of carbon black, silica, clay, resin and curatives.
4. The material constant, M^{**}, is a function of strain rates, temperatures, number of cycles and material compositions.
5. The other material constant, K^*, is independent of temperatures strain rates, strain levels, number of cycles and material compositions.

Acknowledgements

The authors acknowledge the financial support provided by DRDO, New Delhi, for carrying out this research work.

Appendix A

Eq. (29) given in the text can be solved as follows.

Performing the integration with respect to the corresponding variables, then summing a geometric series and rearranging Eq. (29), we obtain the stress at any point in the first cycle

$$S_0^{K^*} = \sum_{k=1}^{k}\left[A_k\left(\frac{t_k^{m_k} - t_{k-1}^{m_k}}{n\omega}\right)\{(N)_k - (N)_{k-1}\} + W_k + Y_k\right] \times \left[(B_k - E_k) - (D_k - G_k)\beta\theta_0\right] + \sum_{k''=k+1}^{k+k_2}(-1)^n\left[A_{k''}t_{k''-1}\left(\frac{d_{k''-1}}{t_{k''-1}^{m_{k''}}} - \frac{d_{k''}}{t_{k''}^{m_{k''}}}\right) + f_{k''} + h_{k''}\right]\left[(B_{k''} - E_{k''}) - (D_{k''} - E_{k''})\beta\theta_0\right] \tag{A1}$$

where

$$A = -\frac{A'' l_0 \{e_0^*(\omega)\}^n}{C_L}$$

$\omega = 2\pi f'$ (f' is the number of cycles per unit of time)

$F = n\omega$

$$H = \sin\left(\frac{n\pi}{2}\right)\cos\delta$$

$$I = \cos\left(\frac{n\pi}{2}\right)\sin\delta$$

$$K = \sin\left(\frac{n\pi}{2}\right)\sin\delta$$

$$L = \cos\left(\frac{n\pi}{2}\right)\cos\delta$$

$$(N)_a = H\sin(Ft_a) + I\sin(Ft_a) + K\cos(Ft_a) - L\cos(Ft_a)$$

$$(d)_a = L\sin(Ft_a) + H\cos(Ft_a) + I\cos(Ft_a) - K\sin(Ft_a)$$

$$b_j' = b_j - 1,\ b_j'' = (1 + 0.5b_j)$$

$$B_k = \frac{e_k^3}{3} + \frac{e_k^2}{2} - \frac{e_{k-1}^3}{3} - \frac{e_{k-1}^2}{2} \text{ (for } b_j' = 1)$$

$$\text{or } \frac{e_k^4}{4} + \frac{2e_k^3}{3} + \frac{e_k^2}{2} - \frac{e_k^4}{4} - \frac{2e_k^3}{3} - \frac{e_k^2}{2} \text{ (for } b_j' = 2)$$

$$\text{or } \frac{1}{b_j' + 2}(e_{k+1} + 1)^{b_j' + 2} - \frac{1}{b_j' + 1}(e_{k+1} + 1)^{b_j' + 1} - \frac{1}{b_j' + 2}(e_k + 1)^{b_j' + 2} + \frac{1}{b_j' + 1}(e_k + 1)^{b_j' + 1} \text{ (for } b_j' > 2)$$

$$E_k = e_{k+1} - \ln(e_{k+1} + 1) - e_k + \ln(e_k + 1) \text{ (for } b_j'' = 1)$$

$$\text{or } \frac{1}{e_{k+1} + 1} + \ln(e_{k+1} + 1) - \frac{1}{e_{k+1}} - \ln(e_k + 1) \text{ (for } b_j'' = 2)$$

$$\text{or } \frac{1}{(b_j'' - 1)(e_{k+1} + 1)^{b_j'' - 1}} - \frac{1}{(b_j'' - 2)(e_{k+1} + 1)^{b_j'' - 2}} - \frac{1}{(b_j'' - 1)(e_k + 1)^{b_j'' - 1}} + \frac{1}{(b_j'' - 2)(e_k + 1)^{b_j'' - 2}} \text{ (for } b_j'' > 2)$$

$$D_k = P_k \ln(e_{k+1} - 1) + \frac{Q_k}{2}\ln(e_{k+1}^2 + e_{k+1} + 1) + \left(R_k - \frac{Q_k}{2}\right)\frac{2}{\sqrt{3}} \arctan\frac{2e_{k+1} + 1}{\sqrt{3}} - P_k \times \ln(e_k - 1) + \frac{Q_k}{2}\ln(e_k^2 + e_k + 1) + \left(R_k - \frac{Q_k}{2}\right)\frac{2}{\sqrt{3}} \arctan\frac{2e_{k+1} + 1}{\sqrt{3}}$$

$$G_k = T_k \ln(e_{k+1} - 1) + \frac{U_k}{2}\ln(e_{k+1}^2 + e_{k+1} + 1) + \left(V_k - \frac{U_k}{2}\right)\frac{2}{\sqrt{3}} \arctan\frac{2e_{k+1} + 1}{\sqrt{3}} - T_k \ln(e_k - 1) + \frac{U_k}{2}\ln(e_k^2 + e_k + 1) + \left(V_k - \frac{U_k}{2}\right)\frac{2}{\sqrt{3}} \arctan\frac{2e_k + 1}{\sqrt{3}}$$

$$X_k = \frac{m_k(m_k - 1)}{2!}\left(\frac{t_k}{t}\right)^2 - \frac{m_k(m_k - 1)(m_k - 2)}{3!}\left(\frac{t_k}{t}\right)^3 + \ldots\infty$$

$$W_k = \text{Imaginary part of } A_k(i)^n(\exp)^{i\delta}\int_{t_{k-1}}^{t_k} t^{m_k} X_k \exp^{ni\omega t} dt$$

$$Y_k = \text{Imaginary part of } A_k(i)^n(\exp)^{i\delta}\left(-m_k t_{k-1} - \frac{m_k}{ni\omega}\right) \times \int_{t_{k-1}}^{t_k} \exp^{ni\omega t}\, dt$$

$$f_{k''} = \text{Imaginary part of } \frac{a_{k''}\exp^{i\delta}}{e_{k'}}$$

$$h_{k''} = \text{Imaginary part of } \frac{b_{k''}\exp^{i\delta}}{e_{k'}}$$

P_k, Q_k, V_k, R_k, T_k and U_k are constants.

References

[1] Mooney MJ. J Appl Phys 1940;11:582.
[2] Flory PJ, Rehner J Jr. J Chem Phys 1943;11:512.
[3] Flory PJ, Erman B. Macromolecules 1982;15:800.
[4] Lal J, Mark JE, editors. Advance in elastomers and rubber elasticity. New York: Plenum Press, 1986.
[5] Arruda EM, Boyce MC. J Mech Phys Solids 1993;41:389.
[6] Besbes S, Bokobza L, Monnerie L, Bahar I, Erman B. Macromolecules 1995;28:231.
[7] Wang S, Mark JE. J Polym Sci, Polym Phys Ed 1992;30:801.
[8] Treloar LRG. The physics of rubber elasticity, 3rd ed. Oxford: Clarendon Press, 1975.
[9] Kuhn W, Grün F. Kolloid Zeitsschrift 1942;101:248.
[10] Kitagawa M, Mori T, Masutani T. J Polym Sci, Polym Phys Ed 1989;27:85.
[11] Koenen JA, Heise B, Kilian HG. J Polym Sci, Polym Phys Ed 1989;27:1235.
[12] Kilian HG, Strauss M, Hamm W. Rubber Chem Technol 1994;67:1.
[13] Charlton DJ, Yang J, Teh KK. Rubber Chem Technol 1994;67:481.
[14] Johnson AR, Quigley CJ, Mead JL. Rubber Chem Technol 1994;67:904.
[15] Padovan J, Paris H, Ma J. Rubber Chem Technol 1995;68:77.
[16] Quigley CJ, Mead J, Johnson AR. Rubber Chem Technol 1995;68:230.
[17] Kawabata S, Yamashita Y, Ooyama H, Yoshida S. Rubber Chem Technol 1995;68:311.

[18] Ferry JD. Viscoelastic properties of polymers, 3rd ed. New York: Wiley, 1980.
[19] Mullins L, Tobin NR. J Appl Polym Sci 1965;9:2993.
[20] Mullins L. Rubber Chem Technol 1969;42:339.
[21] Harwood JAC, Payne AR. J Appl Polym Sci 1966;10:1203.
[22] Harwood JAC, Payne AR, Whittaker RE. Rubber Chem Technol 1971;44:690.
[23] Medalia AI. Rubber Chem Technol 1978;51:436.
[24] Meinecke EA, Taftaf MI. Rubber Chem Technol 1988;61:534.
[25] Roland CM. Rubber Chem Technol 1989;62:880.
[26] Santangelo PG, Roland CM. Rubber Chem Technol 1992;65:965.
[27] Santangelo PG, Roland CM. Rubber Chem Technol 1995;68:124.
[28] Yang T, Chen Y. J. Polym Sci, Part B, Polym Phys 1982;20:1437.
[29] Kar KK, Bhowmick AK. J. Appl Polym Sci 1997;65:1429.
[30] Kar KK, Bhowmick AK. J. Appl Polym Sci 1997;64:1541.
[31] McCallion H, Davies DM. Rubber Chem Technol 1957;30:1045.
[32] Greener J, Tsou AH, Ng KC, Chen WA. J Polym Sci Polym Phys Ed 1991;29:843.
[33] Leblans PJR, Bastiaansen CWM. J Polym Sci, Polym Phys Ed 1989;27:1009.
[34] MacKenzie CI, Scanlan J Polymer 1984;25:559.
[35] Kar KK, Bhowmick AK. Polym Eng Sci 1998;38:38.
[36] Eirich FR. Science and technology of rubber, 1st ed. London: Academic Press, 1978.
[37] Caruthers JM, Cohen RE, Medalia AI. Rubber Chem. Technol. 1976;49:1076.
[38] Brandrup J, Immergut EH. In: Polymer handbook, 3rd ed. New York: Wiley, 1989.